Extracting work from random collisions: A model of a quantum heat engine

Vahid Shaghaghi [1,2], G. Massimo Palma [3,4] and Giuliano Benenti [1,2,4]

[1]*Center for Nonlinear and Complex Systems, Dipartimento di Scienza e Alta Tecnologia, Università degli Studi dell'Insubria, via Valleggio 11, 22100 Como, Italy*

[2]*Istituto Nazionale di Fisica Nucleare, Sezione di Milano, via Celoria 16, 20133 Milano, Italy*

[3]*Dipartimento di Fisica e Chimica–Emilio Segrè, Università degli Studi di Palermo, via Archirafi 36, I-90123 Palermo, Italy*

[4]*NEST, Istituto Nanoscienze-CNR, Piazza S. Silvestro 12, 56127 Pisa, Italy*

(Received 25 November 2021; revised 26 January 2022; accepted 8 February 2022; published 1 March 2022)

We study the statistical distribution of the ergotropy and of the efficiency of a single-qubit battery ad of a single-qubit Otto engine, respectively fueled by random collisions. The single qubit, our working fluid, is assumed to exchange energy with two reservoirs: a nonequilibrium "hot" reservoir and a zero-temperature cold reservoir. The interactions between the qubit and the reservoirs are described in terms of a collision model of open system dynamics. The qubit interacts with the nonequilibrium reservoir (a large ensemble of qudits all prepared in the same pure state) via random unitary collisions and with the cold reservoir (a large ensemble of qubits in their ground state) via a partial swap. Due to the random nature of the interaction with the hot reservoir, fluctuations in ergotropy, heat, and work are present, shrinking with the size of the qudits in the hot reservoir. While the mean, "macroscopic" efficiency of the Otto engine is the same as in the case in which the hot reservoir is a thermal one, the distribution of efficiencies does not support finite moments, so that the mean of efficiencies does not coincide with the macroscopic efficiency.

DOI: 10.1103/PhysRevE.105.034101

I. INTRODUCTION

The development of quantum technologies [1] is pushing the realm of thermodynamics to nanoscale heat engines [2–7]. Here the working fluid can be a particle with discrete energy levels, or in the extreme case even a single qubit. Such setups challenge the validity of thermodynamic concepts and raise fundamental questions related to the discreteness of energy levels, the relevance of quantum coherences, the (possibly strong) coupling to nonequilibrium reservoirs [8–20], and the same definition of heat and work, to name but a few.

Collision models [21–31] (see [32] for a succinct entry point to this framework and [33] for an extensive review) are an important tool for quantum thermodynamics, as they can be used to conveniently model the interaction with reservoirs as unitary transformations, even in the regime of strong system-reservoir coupling. It is then possible to address fundamental problems like the relaxation to equilibrium, the link between information and thermodynamics, the efficiency of thermodynamic cycles in multilevel engines [34], quantum batteries charging [35,36], and non-Markovian effects.

In this work, we consider a particular kind of nonequilibrium, "hot" reservoir, whose interaction with the working fluid is modeled by random collisions [37–41]. Such possibility is quite appealing since by definition random collisions are a "cheap" resource, meaning that no control of type and duration of system-environment interaction is needed. Here the question is whether random collisions, which enhance coherences in the qubit system, can be exploited as a useful resource to perform quantum thermodynamic tasks.

More specifically, we consider a working medium consisting of a single qubit, alternating collisions with a hot, nonequilibrium reservoir and a cold, thermal reservoir. The nonequilibrium reservoir is a nonthermal reservoir, which exchanges energy and coherences with the system. The collisions with the hot reservoir, consisting of qudits, are modeled as random unitaries, while the collisions with the qubits of the cold reservoir are, as usual in the literature, modeled by partial swap operations. In this protocol, the qubit acts as a quantum battery [42] (see [43,44] for reviews), which is charged (discharged) via collisions with the hot (cold) reservoir. We fully characterize the process by looking at the statistical distribution of the ergotropy after each collision. Such distribution exhibits strong fluctuations, due to the random nature of collisions with the hot reservoir, which is reflected in fluctuations in the energy and coherences transferred to the system after each collision. On the other hand, the size of fluctuations shrinks with the dimension μ of the qudits of the "hot" reservoir, and the behavior of a standard, high-temperature thermal reservoir is recovered in the limit $\mu \to \infty$.

We also analyze the impact of the nonequilibrium reservoir on the performance of a quantum Otto engine. We show that the macroscopic mean efficiency of this quantum engine after many cycles, defined as the ratio of the average work per cycle over the average input heat, is the same as for a standard quantum Otto cycle (i.e., with a high-temperature reservoir rather than the nonequilibrium one). On the other hand, fluctuations in work and heat, whose size depends on the dimensionality of the qudits in the nonequilibrium reservoir, imply that that the efficiency for a single cycle is a fluctuating

quantity, We derive the distribution $p(\eta)$ of the single-cycle efficiencies and show that it has a power-law decay with a universal exponent, $p(\eta) \propto \eta^{-2}$ for $\eta \to \pm\infty$. Consequently, such distribution does not support finite moments, so that the mean of efficiencies does not coincide with the macroscopic efficiency.

II. ERGOTROPY FLOW

A. Charge and discharge of the single-qubit battery

Let us first analyze the process of charging and discharging of a single-qubit battery interacting with two reservoirs. The qubit is charged via an exchange of energy—and coherence—with a hot, nonequilibrium, reservoir consisting of a large number of qudits (each belonging to a Hilbert space of dimension μ), all identically prepared in a pure state described by the density operator $\hat{\chi}$. The qubit interacts with such reservoir via a sequence of pairwise random collisions with the individual qudits of the environment. Such collisions are modeled as a random unitary $\hat{\mathcal{R}}(L)$ ($L = 2\mu$ is the dimension of the joint qubit-qudit Hilbert space), drawn from the invariant Haar measure on the unitary group $U(L)$ and conveniently parametrized in terms of the Hurwitz representation [45–47] (for completeness, the procedure is summarized in Appendix A). It is important to note that such collisions are not "weak", i.e., they can strongly change both the energy and the coherences of the single-qubit battery. We also note that the initial state $\hat{\chi}$ of the hot environment qudits is irrelevant after averaging over purely random collisions. Therefore, it does not affect either the averages or the distributions shown in this paper.

The battery then dumps its energy into a cold reservoir, consisting of a large number of qubits, all identically prepared in a thermal state $\hat{\vartheta}$. Again the system-environment interaction takes place via a sequence of pairwise collisions between the battery qubit and the environment qubits. We assume each collision to be described by a (unitary) partial swap operation:

$$\hat{\mathcal{P}}(\alpha) = \cos\alpha \hat{I} + i \sin\alpha \hat{\mathcal{S}} \quad \left(0 \leqslant \alpha \leqslant \frac{\pi}{2}\right), \tag{1}$$

where $\hat{\mathcal{S}}$ is the swap operator: $\hat{\mathcal{S}}(|\phi\rangle \otimes |\psi\rangle) \equiv |\psi\rangle \otimes |\phi\rangle$. If the system state before a collision with the cold reservoir is $\hat{\varrho}$, then after the collision it is

$$\hat{\varrho}\,' = \cos^2\alpha\, \hat{\varrho} + \sin^2\alpha\, \hat{\vartheta} + i \sin\alpha \cos\alpha [\hat{\vartheta}, \hat{\varrho}], \tag{2}$$

where we have traced over the environment degrees of freedom. Note that, in the case of complete swap, i.e., $\alpha = \frac{\pi}{2}$, the qubit state $\hat{\varrho}\,'$ after the collision is a Gibbs state, which is, as we will explain shortly, passive. In that case, battery discharging is complete. We also note that, due to the random nature of collisions with the hot reservoir, the qubit system after colliding with such reservoir can be found in a state with an energy smaller than the energy of the cold reservoir qubits. In such instances, the partial swap does not dump energy into the cold reservoir but rather extracts energy from it. The expected working of a cold reservoir is, however, recovered after ensemble averaging (over the random collisions) or time averaging (over a sequence of cycles of the battery).

Since the hot reservoir is a nonthermal environment consisting of pure states interacting with the battery via random unitaries, as we mentioned already the system-environment collisions will modify the battery coherences. In this scenario a convenient quantity to analyze the flux of energy from the hot to the cold reservoir is the battery ergotropy [48], i.e., the maximum amount of work that can be extracted from the battery via a suitable unitary evolution $\hat{\mathcal{U}}$ (in our case a single-qubit non-dissipative evolution).

For a system described by a density operator $\hat{\varrho}$ and Hamiltonian $\hat{H}$, the ergotropy is defined as

$$\mathcal{E}(\hat{\varrho}, \hat{H}) = \mathrm{Tr}(\hat{\varrho}\hat{H}) - \min[\mathrm{Tr}(\hat{\mathcal{U}}\hat{\varrho}\,\hat{\mathcal{U}}^\dagger \hat{H})], \tag{3}$$

where the minimum is taken over all possible unitary transformations $\hat{\mathcal{U}}$. Given the state $\hat{\varrho} = \sum_n r_n |r_n\rangle\langle r_n|$ and the Hamiltonian $\hat{H} = \sum_n \varepsilon_n |\varepsilon_n\rangle\langle\varepsilon_n|$, with $r_0 \geqslant r_1 \geqslant \ldots$, and $\varepsilon_0 \leqslant \varepsilon_1 \leqslant \ldots$, there is a unique state

$$\hat{\pi} = \hat{\mathcal{U}}\hat{\varrho}\,\hat{\mathcal{U}}^\dagger = \sum_n r_n |\epsilon_n\rangle\langle\epsilon_n|$$

which minimizes $\mathrm{Tr}(\hat{\mathcal{U}}\hat{\varrho}\,\hat{\mathcal{U}}^\dagger\hat{H})$. The state $\hat{\pi}$ is called passive, since it cannot deliver any work via the above unitary dynamics.

Given the Bloch sphere representation of the qubit state, $\hat{\varrho} = \frac{1}{2}(\hat{I} + \mathbf{r}\cdot\hat{\boldsymbol{\sigma}})$, with $\mathbf{r} = (x, y, z)$ the Bloch vector and $\hat{\boldsymbol{\sigma}} = (\hat{\sigma}_x, \hat{\sigma}_y, \hat{\sigma}_z)$ the vector of Pauli matrices, and the Hamiltonian $\hat{H} = \frac{1}{2}\Delta\hat{\sigma}_z$, we have $\mathcal{E} = \Delta(r + z)$, where $r = \sqrt{x^2 + y^2 + z^2}$ is the length of the Bloch vector. The qubit acts as a quantum battery, which can be charged or discharged via unitary interactions (collisions) with qubits (or qudits) of the environment.

We consider a sequence of charging-discharging cycles. The reservoirs are assumed to be so large that the system never collides twice with the same environment qudit (qubit). We can have a pictorial view of the model by considering a single qubit colliding in sequence with the individual qudits (qubits) of two long chains, corresponding to the hot and cold reservoirs, respectively. If $\hat{\varrho}_n$ denotes the system's density operator after n cycles (collisions with each reservoir), we have the map

$$\hat{\varrho}_{n+1} = \mathrm{Tr}_{\mathrm{HC}}\{\hat{\mathcal{P}}\hat{\mathcal{R}}(\hat{\varrho}_n \otimes \hat{\chi} \otimes \hat{\theta})\hat{\mathcal{R}}^\dagger\hat{\mathcal{P}}^\dagger\}, \tag{4}$$

where the trace is over both [hot (H) and cold (C)] reservoirs.

B. Statistical distribution of the battery ergotropy

We numerically investigate the mean and the statistical distribution of ergotropy, as a function of the number of collisions with the reservoirs. Hereafter we set the state of the cold reservoir qubits as $\hat{\theta} = |\downarrow\rangle\langle\downarrow|$. This ideal case of a zero-temperature reservoir leads, after a collision with complete swap, to the passive state with the lowest energy (i.e., ground state energy) for the system.

We first consider the case in which the hot reservoir consists of qubits ($\mu = 2$). Initially the system is prepared in a pure state (as discussed above, which one is irrelevant when averaging over random collisions). In Fig. 1 we show the numerically generated histograms of statistical distributions of the system ergotropies, after each of the first three collisions with the hot and the cold reservoir. Hereafter, we consider 10^4 trajectories, i.e., each one with random unitaries drawn from the invariant Haar measure on the unitary group $U(L = 2\mu) = 4$. Note that the ergotropy $\mathcal{E} = \Delta(r + z)$ can vary in

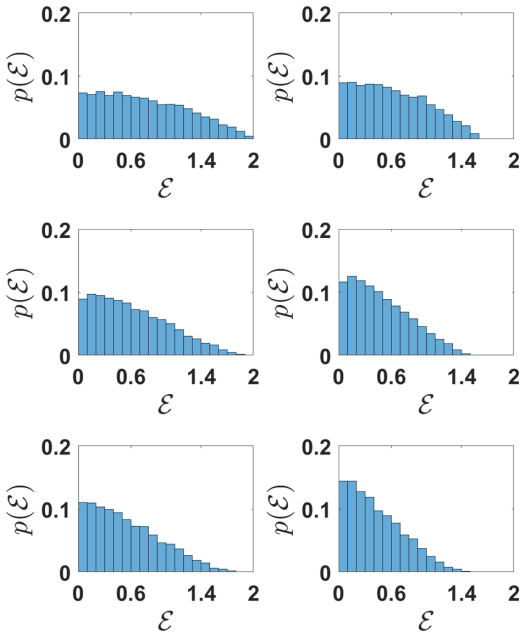

FIG. 1. Histograms showing the statistical distribution of the ergotropies of the system, after collisions with the hot reservoir (left panels) or the cold reservoir (right panels). From top to bottom: distributions after the first, the second, and the third collision with the (hot or cold) reservoir. The hot reservoir consists of qubits ($\mu = 2$); the swap parameter $\alpha = \frac{\pi}{10}$.

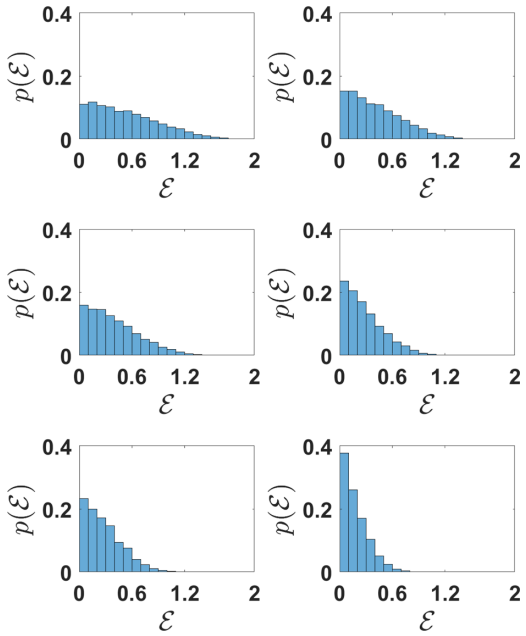

FIG. 3. Histograms showing the statistical distribution of the ergotropies of the system, after $n = 6$ cycles, a collision with the hot reservoir (left panels), and a further collision with the cold reservoir (right panels). From top to bottom: qudits of dimension $\mu = 2$, 4, and 8. Swap parameter $\alpha = \frac{\pi}{10}$.

the range $0 \leqslant \mathcal{E} \leqslant 2$, since the length of the Bloch vector $r \leqslant 1$. The ergotropy distribution can achieve higher values after collisions with the nonequilibrium reservoir, while the distribution shrinks after the battery dumps energy colliding with the cold reservoir.

We then show in Fig. 2 the mean ergotropy as a function of the number t of collisions, for different values of the swap parameter α. We can see that a periodic steady state is approached, with a period of two collisions, one with the hot and one with the cold reservoir. The value of α affects the time needed to practically achieve the periodic steady state, as well as the working of the quantum battery. Indeed, the effectiveness of the discharging process increases with the swap parameter, and a passive state is obtained for the limiting case of complete swap, $\alpha = \frac{\pi}{2}$.

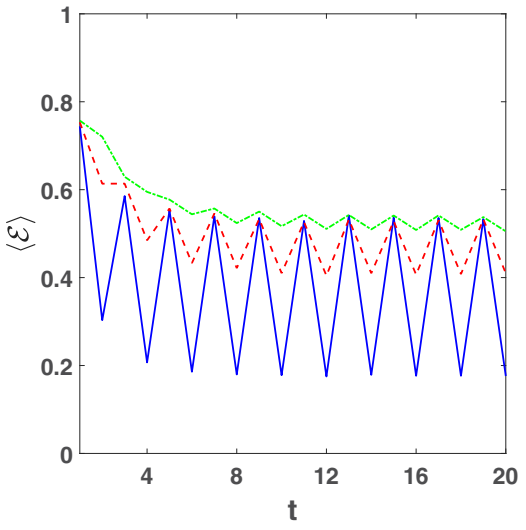

FIG. 2. Ensemble-averaged ergotropy as a function of the number of collisions (alternating collisions with the hot, $\mu = 2$, and the cold reservoir). Swap parameter $\alpha = \frac{\pi}{20}$ (top green line), $\frac{\pi}{10}$ (middle red line), and $\frac{\pi}{5}$ (bottom blue line).

In what follows, we change the dimension μ of the qudits in the hot reservoir. The statistical distribution of the ergotropies is shown in Fig. 3 after six cycles, so that for the used value of the swap parameter ($\alpha = \frac{\pi}{10}$) the periodic steady state is in practice achieved. We can see that the distribution shrinks with increasing the dimension μ. The mean ergotropy, shown in Fig. 4 as a function of the number of collisions, is smaller at larger μ. Indeed, in the limit $\mu \to \infty$ the nonequilibrium reservoir acts as an infinite-temperature reservoir, leading the system qubit after each collision to the completely mixed thermal state $\varrho = \frac{I}{2}$, for which the ergotropy vanishes.

III. A QUANTUM OTTO ENGINE FUELED BY RANDOM COLLISIONS

In the previous section we have introduced a model where the hot reservoir is a nonequilibrium reservoir, which can enhance coherences in the working medium, which in our case is a qubit system. It is therefore appealing to investigate whether these coherences could be used to improve the performance of a heat engine. On a more fundamental level, the key question is whether a proper thermodynamic description in terms of a heat engine is possible, for the smallest-size working medium, a qubit, fueled by a nonequilibrium reservoir modeled via

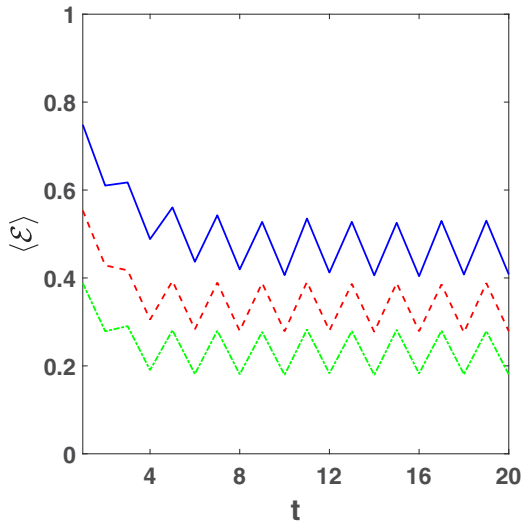

FIG. 4. Ensemble-averaged ergotropy as a function of the number of collisions (alternating collisions with the hot and the cold reservoir). Swap parameter $\alpha = \frac{\pi}{10}$, and qudits of dimension $\mu = 2$ (top blue line), 4 (middle red line), and 8 (bottom green line).

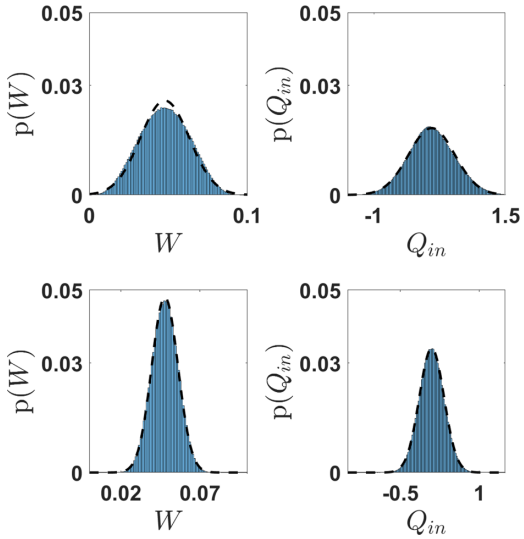

FIG. 5. Histogram showing the statistical distribution of work W (left panels) and input heat $Q_{\rm in}$ (right panels) for the Otto cycle described in the text. The hot reservoir consists of qudits of dimension $\mu = 2$ (top panels) and 8 (bottom panels). Swap parameter $\alpha = \frac{\pi}{10}$. Qubit gaps during the cycle: $\Delta_1 = 2$, $\Delta_2 = 1$. Dashed lines show Gaussian fits.

purely random collisions. To address these questions, we consider the paradigmatic model of a quantum Otto cycle [34], consisting of four strokes.

Stroke A. The system, initially in the state $\hat{\varrho}$, interacts with the hot, nonequilibrium reservoir, while its Hamiltonian remains unchanged, $\hat{H}_1 = \frac{1}{2}\Delta_1\hat{\sigma}_z$ ($\Delta_1 > 0$). The collision is modeled as a random unitary transformation, after which the system density matrix becomes $\hat{\varrho}'$. The heat absorbed by the system is then given by

$$Q_{\rm in} = {\rm Tr}(\hat{H}_1\hat{\varrho}') - {\rm Tr}(\hat{H}_1\hat{\varrho}) = \tfrac{1}{2}\Delta_1(z' - z), \tag{5}$$

where z and z' are the z components of the Bloch vectors of $\hat{\varrho}$ and of $\hat{\varrho}'$, respectively.

Stroke B. The system is decoupled from the hot reservoir and its Hamiltonian is adiabatically changed up to $\hat{H}_2 = \frac{1}{2}\Delta_2\hat{\sigma}_z$ (with $\Delta_1 > \Delta_2 > 0$), whereas the system density matrix $\hat{\varrho}'$ remains unchanged. The work performed by the system is given by

$$W_{\rm out} = {\rm Tr}(\hat{H}_1\hat{\varrho}') - {\rm Tr}(\hat{H}_2\hat{\varrho}') = \tfrac{1}{2}z'(\Delta_1 - \Delta_2). \tag{6}$$

Stroke C. The system Hamiltonian remains unchanged, and the interaction of the system with the cold, thermal reservoir is modeled by a partial swap collision, after which the system density matrix becomes $\hat{\varrho}''$. The heat absorbed by the system (on average negative) is

$$Q_{\rm out} = {\rm Tr}(\hat{H}_2\hat{\varrho}'') - {\rm Tr}(\hat{H}_2\hat{\varrho}') = \tfrac{1}{2}\Delta_2(z'' - z'). \tag{7}$$

Stroke D. The system is decoupled from the cold reservoir and its Hamiltonian adiabatically returns to $\hat{H}_1 = \frac{1}{2}\Delta_1\hat{\sigma}_z$, whereas the system density matrix $\hat{\varrho}''$ remain unchanged. The work performed by the system (on average negative) is

$$W_{\rm in} = {\rm Tr}(\hat{H}_2\hat{\varrho}'') - {\rm Tr}(\hat{H}_1\hat{\varrho}'') = \tfrac{1}{2}z''(\Delta_2 - \Delta_1). \tag{8}$$

We point out that each single realization of the Otto cycle is not strictly speaking a true cycle since in general the final state $\hat{\varrho}''$ is different from the initial state $\hat{\varrho}$. Additionally, due to the strong fluctuations induced by the random collisions with the hot reservoir, even the signs of the contributions of the various strokes to work and heat are not always in agreement with those expected for a standard quantum Otto engine. For instance, the distribution of input heat $Q_{\rm in}$ exhibits events where $Q_{\rm in} < 0$ (see Fig. 5). However, as discussed below, by a suitable ensemble average it is possible to define a "macroscopic" efficiency and recover the standard result expected for a quantum Otto engine.

If we use the standard formula for the efficiency η of a heat engine we obtain

$$\eta = \frac{W}{Q_{\rm in}} = \frac{z' - z''}{z' - z}\left(1 - \frac{\Delta_2}{\Delta_1}\right), \tag{9}$$

where $W = W_{\rm in} + W_{\rm out}$. This formula can lead to negative values for the efficiency (see Fig. 6). Indeed, due to the randomness of the interaction process with the nonequilibrium bath we can have cycles where the output work is negative. The treatment of efficiency as a fluctuating quantity is quite natural for small-scale engines, operating in the presence of highly fluctuating energy exchanges with the environment. In this case, the fluctuating efficiency can even exceed the Carnot limit [49], in correspondence with rare events leading to negative entropy production. On the other hand, fluctuation theorems [50] ensure that standard thermodynamics is recovered after proper averaging. In our model, after ensemble averaging, we obtain a periodic steady state (with the period of the Otto cycle), and therefore $\langle\hat{\varrho}''\rangle = \langle\hat{\varrho}\rangle$ ($\langle\cdots\rangle$ denotes ensemble averaging). Consequently we have $\langle z''\rangle = \langle z\rangle$, which leads to the standard Otto cycle efficiency [34]:

$$\eta_m = \frac{\langle W\rangle}{\langle Q_{\rm in}\rangle} = 1 - \frac{\Delta_2}{\Delta_1}. \tag{10}$$

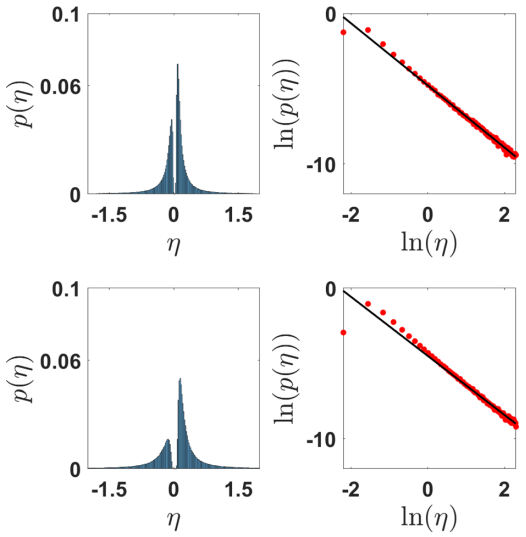

FIG. 6. Histogram showing the statistical distribution of the efficiency η, for dimension of the hot reservoir qudits $\mu = 2$ (top panels) and 8 (bottom panels), for the same parameter values as in Fig. 5. Right panels show the $\eta > 0$ data in log-log scale (natural logarithms), with power-law fits $p(\eta) \propto 1/\eta^{\alpha}$, with $\alpha = -2.00$ (top) and -1.97 (bottom).

This macroscopic efficiency can be obtained after averaging work and input heat over a large number of cycles and/or over an ensemble of random collisions. After ensemble averaging, the nonequilibrium reservoir acts as an infinite-temperature reservoir, leaving the system in a fully unpolarized state, and therefore the ideal Carnot efficiency is equal to 1. This limit is achieved when the gap ratio $\Delta_2/\Delta_1 \to 0$.

While efficiency assumes a clear thermodynamic meaning only after one of these two averages, it is nevertheless interesting, when considering the engine constancy, to investigate efficiency fluctuations. In what follows, we shall perform such study.

We first consider the statistical distributions of work W and input heat $Q_{\rm in}$, shown in Fig. 5. Hereafter, histograms are constructed on 10^6 cycles. It can be seen that all histrograms are nicely fitted by a Gaussian distribution, of width decreasing with increasing the dimension μ of the qudits in the nonequilibrium reservoirs. More precisely, we have seen that the standard deviations of both W and $Q_{\rm in}$ decrease, for a given swap parameter α, as $1/\sqrt{\mu}$. We have also checked the validity of the Gaussian fit for other values of α, with the standard deviation of the work distribution increasing with α.

Finally, we consider the efficiency distributions, shown (for the cases of Fig. 5) in Fig. 6. Assuming, as confirmed by numerical simulations, Gaussian distributions for both W and $Q_{\rm in}$, we obtain a ratio distribution $p(\eta)$ for $\eta = W/Q_{\rm in}$ known from the literature (see Appendix B for details). Such distribution predicts a power-law decay with a universal exponent, $p(\eta \to \pm\infty) \propto \eta^{-2}$, consistent with the power-law fits shown in the right plots of Fig. 6. Finally, we point out that a decay $p(\eta \to \pm\infty) \propto \eta^{-2}$ implies that moments of any order of $p(\eta)$ are not finite. In particular, the mean efficiency $\langle\eta\rangle$ is not finite and therefore does not coincide with the macroscopic efficiency $\eta_m = \langle W\rangle/\langle Q_{\rm in}\rangle$ [51].

IV. CONCLUSIONS

In this paper, we have characterized the working of the smallest-size quantum medium, i.e., a single qubit, when operating either as a quantum battery or as a working fluid in a quantum Otto cycle. While we have considered a standard, thermal reservoir as a cold bath, we have modeled the action of the hot, nonequilibrium reservoir via random collision. This setup allows one to extract work, with the mean, macroscopic efficiency equal to that obtained with the hot reservoir being a thermal one. On the other hand, fluctuations in the output work and in the heat absorbed from the hot, nonequilibrium reservoir play a very important role, due to the random nature of collisions. Consequently, also the single-cycle efficiency, as naturally happens when dealing with microscopic systems, is a fluctuating quantity. In particular, the distribution of efficiencies does not afford finite moments of any order, so that the mean of efficiencies does not coincide with the macroscopic efficiency.

It is interesting to remark that random collisions, that is, operations which by definition do not require specific control of the unitary transformations, can be used to extract work. It would be interesting to explore such possibility in real, noisy intermediate-scale quantum hardware or in quantum annealers.

ACKNOWLEDGMENTS

We acknowledge support by the INFN through the project QUANTUM. V.S. acknowledges support from a fellowship from the ICTP Programme for Training and Research in Italian Laboratories, Trieste, Italy.

APPENDIX A: HURWITZ PARAMETRIZATION FOR THE UNITARY GROUP

In this Appendix, following Refs. [45–47], we summarize for completeness the main steps taken to draw a random unitary transformation from the invariant Haar measure for the unitary group $U(L)$. We start by defining the unitary transformation $E_n(\varphi, \psi, \chi)$, which differs from the identity only in a 2×2 block, whose matrix elements read

$$(E_n)_{nn} = e^{i\psi}\cos\varphi, \quad (E_n)_{n,n+1} = e^{i\chi}\sin\varphi,$$
$$(E_n)_{n+1,n} = -e^{-i\chi}\sin\varphi, \quad (E_n)_{n+1,n+1} = e^{-i\psi}\cos\varphi. \quad \text{(A1)}$$

Each unitary transformation in $U(L)$ is then decomposed as

$$U = U_1 U_2 U_3 \cdots U_{L-1}, \quad \text{(A2)}$$

where

$$\begin{aligned} U_1 &= E_{L-1}(\varphi_{01}, \psi_{01}, \chi_1), \\ U_2 &= E_{L-2}(\varphi_{12}, \psi_{12}, 0)E_{L-1}(\varphi_{02}, \psi_{02}, \chi_2), \\ U_3 &= E_{L-3}(\varphi_{23}, \psi_{23}, 0)E_{L-2}(\varphi_{13}, \psi_{13}, 0)E_{L-1}(\varphi_{03}, \psi_{03}, \chi_3), \\ &\vdots \\ U_{L-1} &= E_1(\varphi_{L-2,L-1}, \psi_{L-2,L-1}, 0)E_2(\varphi_{L-3,L-1}, \psi_{L-3,L-1}, 0)\cdots E_{L-1}(\varphi_{0,L-1}, \psi_{0,L-1}, \chi_{L-1}), \end{aligned} \tag{A3}$$

with the Euler angles in the range

$$0 \leqslant \varphi_{rs} \leqslant \frac{\pi}{2}, \quad 0 \leqslant \psi_{rs} < 2\pi, \quad 0 \leqslant \chi_s < 2\pi. \tag{A4}$$

The (normalized) Haar measure for the unitary group $U(L)$, invariant with respect to the composition of unitary matrices, is

$$dU = \frac{2^{1-L}\pi}{\prod_{k=1}^{L} \frac{\pi^k}{\Gamma(k)}} \prod_{r,s} \cos\varphi_{rs}(\sin\varphi_{rs})^{2r+1} d\varphi_{rs} d\psi_{rs} \prod_s d\chi_s,$$
$$s = 1, 2, \ldots, L-1, \quad r = 0, 1, \ldots, s-1. \tag{A5}$$

In order to generate unitary random matrices for numerical simulations, we note that the Haar measure (A5) implies that the azimuthal angles ψ_{rs}, χ_s must be generated with a uniform distribution in their range $[0, 2\pi[$. In order to generate the nonuniform distribution of the polar angles φ_{rs}, we use the auxiliary variables ξ_{rs}, uniformly distributed in the interval [0,1], defined by the relation

$$\varphi_{rs} = \sin^{-1}(\xi_{rs})^{1/(2r+2)}. \tag{A6}$$

APPENDIX B: EFFICIENCY PROBABILITY DISTRIBUTION

Assuming that the work $W = W_{\text{in}} + W_{\text{out}}$ and the input heat Q_{in} are independent Gaussian random variables, we can obtain an analytical expression the efficiency probability distribution function $p(\eta)$. Following [54,55], we have

$$\begin{aligned} p(\eta) &= \int dW\, dQ\, \delta\left(\eta - \frac{W}{Q}\right) p(W, Q) \\ &= \int_{-\infty}^{\infty} |Q| p(\eta Q, Q) dQ, \end{aligned} \tag{B1}$$

where $p(W, Q)$ is the joint probability distribution function for W and Q_{in} (to simplify writing, hereafter we set $Q \equiv Q_{\text{in}}$):

$$p(W, Q) = \frac{1}{2\pi\sigma_Q\sigma_w} \exp\left\{-\frac{1}{2}\left[\frac{(W-\mu_w)^2}{\sigma_W^2} + \frac{(Q-\mu_Q)^2}{\sigma_Q^2}\right]\right\}, \tag{B2}$$

with μ_W, μ_Q and σ_W, σ_Q mean and standard deviation of the Gaussian distributions for W and Q. After straightforward integration we obtain

$$\begin{aligned} p(\eta) = \frac{d(\eta)b(\eta)}{2\sqrt{2\pi}\sigma_Q\sigma_w a(\eta)^3}\Bigg[2 - \operatorname{erf}\left(-\frac{b(\eta)}{\sqrt{2}a(\eta)}\right) \\ + \operatorname{erf}\left(\frac{b(\eta)}{\sqrt{2}a(\eta)}\right)\Bigg] + \frac{e^{-c/2}}{\pi\sigma_Q\sigma_w a(\eta)^2}, \end{aligned} \tag{B3}$$

where we have introduced

$$\begin{aligned} a(\eta) &= \sqrt{\frac{\eta^2}{\sigma_w^2} + \frac{1}{\sigma_Q^2}}, \quad b(\eta) = \frac{\mu_w\eta}{\sigma_w^2} + \frac{\mu_Q}{\sigma_Q^2}, \\ c &= \frac{\mu_w^2}{\sigma_w^2} + \frac{\mu_Q^2}{\sigma_Q^2}, \quad d(\eta) = \exp\left\{\frac{b^2(\eta) - ca^2(\eta)}{2a^2(\eta)}\right\}. \end{aligned} \tag{B4}$$

This distribution has power-law tails: $p(\eta \to \pm\infty) \propto \eta^{-2}$.

[1] G. Benenti, G. Casati, D. Rossinii, and G. Strini, *Principles of Quantum Computation and Information:* (A Comprehensive Textbook) (World Scientific, Singapore, 2019).

[2] R. Kosloff, Entropy **15**, 2100 (2012).

[3] D. Gelbwaser-Klimovsky, W. Niedenzu, and G. Kurizki, Adv. At., Mol., Opt. Phys. **64**, 329 (2015).

[4] S. Vinjanampathy and J. Anders, Contemp. Phys. **57**, 545 (2016).

[5] B. Sothmann, R. Sánchez, and A. N. Jordan, Nanotechnology **26**, 032001 (2015).

[6] J. Goold, M. Huber, A. Riera, L. del Rio, and P. Skrzypczyk, J. Phys. A: Math. Theor. **49**, 143001 (2016).

[7] G. Benenti, G. Casati, K. Saito, and R. S. Whitney, Phys. Rep. **694**, 1 (2017).

[8] M. O. Scully, M. S. Zubairy, G. S. Agarwal, and H. Walther, Science **299**, 862 (2003).

[9] X. L. Huang, T. Wang, and X. X. Yi, Phys. Rev. E **86**, 051105 (2012).

[10] O. Abah and E. Lutz, Europhys. Lett. **106**, 20001 (2014).

[11] J. Roßnagel, O. Abah, F. Schmidt-Kaler, K. Singer, and E. Lutz, Phys. Rev. Lett. **112**, 030602 (2014).

[12] A. Ü. C. Hardal and Ö. E. Müstecaplioglu, Sci. Rep. **5**, 12953 (2015).

[13] W. Niedenzu, D. Gelbwaser-Klimovsky, A. G. Kofman. and G. Kurizki, New J. Phys. **18**, 083012 (2016).

[14] G. Manzano, F. Galve, R. Zambrini, and J. M. R. Parrondo, Phys. Rev. E **93**, 052120 (2016).

[15] J. Klaers, S. Faelt, A. Imamoglu, and E. Togan, Phys. Rev. X **7**, 031044 (2017).

[16] B. K. Agarwalla, J.-H. Jiang, and D. Segal, Phys. Rev. B **96**, 104304 (2017).

[17] W. Niedenzu, V. Mukherjee, A. Ghosh, A. G. Kofman. and G. Kurizki, Nat. Commun. **9**, 165 (2018).

[18] C. Cherubim, F. Brito, and S. Deffner, Entropy **21**, 545 (2019).
[19] J. Wang, J. He, and Y. Ma, Phys. Rev. E **100**, 052126 (2019).
[20] C. M. Latune, I. Sinayskiy, and F. Petruccione, Eur. Phys. J.: Spec. Top. **230**, 841 (2021).
[21] J. Rau, Phys. Rev. **129**, 1880 (1963).
[22] R. Alicki and K. Lendi, *Quantum Dynamical Semigroups and Applications*, Lecture Notes in Physics (Springer-Verlag, Berlin, 1987).
[23] V. Scarani, M. Ziman, P. Štelmachovic, N. Gisin, and V. Bužek, Phys. Rev. Lett. **88**, 097905 (2002).
[24] M. Ziman, P. Štelmachovic, V. Bužek, M. Hillery, V. Scarani, and N. Gisin, Phys. Rev. A **65**, 042105 (2002).
[25] M. Ziman and V. Bužek, Phys. Rev. A **72**, 022110 (2005).
[26] G. Benenti and G. M. Palma, Phys. Rev. A **75**, 052110 (2007).
[27] V. Giovannetti and G. M. Palma, Phys. Rev. Lett. **108**, 040401 (2012).
[28] S. Lorenzo, R. McCloskey, F. Ciccarello, M. Paternostro, and G. M. Palma, Phys. Rev. Lett. **115**, 120403 (2015).
[29] P. Strasberg, G. Schaller, T. Brandes, and M. Esposito, Phys. Rev. X **7**, 021003 (2017).
[30] G. De Chiara, G. Landi, A. Hewgill, B. Reid, A. Ferraro, A. J. Roncaglia, and M. Antezza, New J. Phys. **20**, 113024 (2018).
[31] M. Pezzutto, M. Paternostro, and Y. Omar, Quantum Sci. Technol. **4**, 025002 (2019).
[32] S. Campbell and B. Vacchini, Europhys. Lett. **133**, 60001 (2021).
[33] F. Ciccarello, S. Lorenzo, V. Giovannetti, and G. M. Palma, Phys. Rep. **954**, 1 (2022).
[34] R. Uzdin and R. Kosloff, New J. Phys. **16**, 095003 (2014).
[35] S. Seah, M. Perarnau-Llobet, G. Haack, N. Brunner, and S. Nimmrichter, Phys. Rev. Lett. **127**, 100601 (2021).
[36] G. Landi, Entropy **23**, 1627 (2021).
[37] C. Pineda and T. H. Seligman, Phys. Rev. A **75**, 012106 (2007).
[38] C. Pineda, T. Gorin, and T. H. Seligman, New J. Phys. **9**, 106 (2007).
[39] A. Akhalwaya, M. Fannes, and F. Petruccione, J. Phys. A: Math. Theor. **40**, 8069 (2007).
[40] G. Gennaro, G. Benenti, and G. M. Palma, Europhys. Lett. **82**, 20006 (2008).
[41] G. Gennaro, G. Benenti, and G. M. Palma, Phys. Rev. A **79**, 022105 (2009).
[42] R. Alicki and M. Fannes, Phys. Rev. E **87**, 042123 (2013).
[43] F. Campaioli, F. A. Pollock, and S. Vinjanampathy, in *Thermodynamics in the Quantum Regime*, edited by F. Binder, L. A. Correa, C. Gogolin, J. Anders, and G. Adesso, Vol. 195 (Springer, Cham, 2018), pp. 207–225.
[44] S. Bhattacharjee and A. Dutta, Eur. Phys. J. B **94**, 239 (2021).
[45] M. Pozniak, K. Zyczkowski, and M. Kus, J. Phys. A: Math. Gen. **31**, 1059 (1998).
[46] Y. S. Weinstein and C. S. Hellberg, Phys. Rev. Lett. **95**, 030501 (2005).
[47] G. Gennaro, Irreversible Dynamics and Entanglement Generation by Random Collisions, Ph.D. thesis, University of Palermo, Italy, 2010.
[48] A. E. Allahverdyan, R. Balian, and T. M. Nieuwenhuizen, Europhys. Lett. **67**, 565 (2004).
[49] G. Verley, M. Esposito, T, Willaert, C. Van den Broeck, Nat. Commun. **5**, 4721 (2014).
[50] M. Campisi, P. Hänggi, and P. Talkner, Rev. Mod. Phys. **83**, 771 (2011).
[51] A similar divergence of the mean efficiency was discussed for phenomenological linear response coupled transport equations [7,52,53] by M. Polettini, G. Verley, and M. Esposito, Phys. Rev. Lett. **114**, 050601 (2015).
[52] H. B. Callen, *Thermodynamics and an Introduction to Thermostatics*, 2nd ed. (Wiley, New York, 1985).
[53] S. R. de Groot and P. Mazur, *Nonequilibrium Thermodynamics* (North-Holland, Amsterdam, 1962).
[54] J. H. Curtiss, Ann. Math. Stat. **12**, 409 (1941).
[55] D. V. Hinkley, Biometrika **56**, 635 (1969).